2021 43rd Annual International Conference of the
IEEE Engineering in Medicine & Biology Society (EMBC)
Oct 31 - Nov 4, 2021. Virtual Conference

Comparison of gold and PEDOT:PSS contacts for high-resolution gastric electrical mapping using flexible printed circuit arrays

Peikai Zhang[1], Jadranka Travas-Sejdic[1], Gregory O'Grady,[2] Peng Du[3]

Abstract — **Motility of the stomach is governed by an electrophysiological event termed gastric slow waves. High-resolution (HR) bioelectrical mapping involves placing array of electrodes over the surface of the stomach to record gastric slow waves. Conductive polymer materials have recently been applied to great effect in cardiology and neurophysiology due to its compliant and biocompatible properties. The aim of this study was to quantify the performance of poly(3,4-ethylenedioxythiophene) doped with poly(styrenesulfonate) (PEDOT:PSS) deposited on a flexible print circuit electrode array for gastric slow wave HR mapping. The Au electrodes were coated with PEDOT:PSS at 1 V and different levels of charges (0.3-1.2 mC). HR mapping alongside standard Au electrodes was performed in three anesthetized pigs. Overall, the PEDOT:PSS electrodes detected both antegrade and retrograde slow wave propagations, with comparable frequency, velocity and signal-to-noise ratio to the Au electrodes. Differences between the two electrodes were noted in terms of amplitude and downstroke gradient. The findings of this study will inform designs of future stretchable and implantable HR mapping electrode arrays for gastrointestinal recording and stimulation therapies.**

Clinical Relevance — **The applications of PEDOT:PSS will allow long-term monitoring and stimulation of the gut.**

I. Introduction

Motility of the gastrointestinal (GI) tract is governed by an electrophysiological activity termed slow waves [1]. In the healthy stomach, gastric slow waves originate from a pacemaker region instead of a node in the proximal stomach, and form successive bands of propagating wavefronts around the lumen of the stomach towards the pylorus [2]. Dysrhythmias of gastric slow waves have been proposed as a sensitive biomarker for detection of a number of clinically challenging conditions, such as gastroparesis, chronic nausea and vomiting, and functional dyspepsia (indigestion) [3].

Conventional high-resolution (HR) mapping of GI slow waves is performed using electrodes in epoxy-embedded resins [4]. The arrays are rigid but offers good signal-to-noise ratio (SNR) due to the stable contact between the AgCl leads and tissue. More recent investigations have utilized the flexible printed circuit (FPC) technique to produce Au coated electrodes embedded in polyamide substrate [5]. The FPC electrodes are mass producible and easy to sterilize for single or repeated applications in human intra-operative studies [6]. While the Au coating theoretically offers less SNR than AgCl coating, a previous investigation has found comparable performance between the two coating materials for GI slow wave recordings [7].

While the FPC electrodes have been adequate in acute clinical studies, a number of significant challenges remain. In particular, the polyamide material is flexible but does not conform well to curved anatomical geometries and the standard coating on FPC induces local immunological response in the GI tissue if implanted. Sustained contact with the tissue is also a problem in long-term studies. Taken together, these limitations associated with FPC electrodes, there is a need for an improved solution to the current HR mapping technique in the GI field.

Conducting (conjugated) polymers (CP) are ideal candidates to be used as active bio-interface for a wide range of medical applications [8], [9]. Under applied potential, CP films readily exchange ions with the biological fluids throughout the bulk of the CP, forming a 3D electronic communication interface with a high volumetric capacitance that translates into a lower electrochemical impedance, necessary for effective communication across the interface. Furthermore, a common CP material, PEDOT:PSS, is biocompatible [10], and its mechanical properties can be tuned to achieve the desirable searchability and adhesion [11].

The main objective of this study was to compare the performance of PEDOT:PSS coating under different electrotechnical deposition settings to the standard Au FPC electrodes. The outcome will inform design and manufacturing of the next generation of HR mapping and multi-modal recording devices for GI electrophysiology and motility.

II. Methods

A. PEDOT:PSS deposition

A previously described FPC electrode (2x16 electrodes; 4 mm inter-electrode spacing; Gen5, FlexiMap, New Zealand) was used as the platform for comparing the performance of Au and PEDOT:PSS electrode contacts (Fig. 1B). A mixed solution containing 0.01 M EDOT and 0.1 M NaPSS in deionized water (Milli-Q 18.2 MΩ cm) was used for the electropolymerisation. 12 electrodes were coated by PEDOT:PSS by applying a constant electrical potential of 1

This work was funded by a Rutherford Discovery Fellowship from the Rutherford Foundation Trust, Catalyst Grant, and Prime Minister's Emerging Scientist Prize administered by the Royal Society Te Apārangi.

1. P Zhang, J Travas-Sejdic are with the Polymer Biointerface Centre, School of Chemical Sciences, The University of Auckland, New Zealand, and The MacDiarmid Institute of Advanced Materials and Nanotechnology, New Zealand

2. G O'Grady is with the Department of Surgery and with Auckland Bioengineering Institute, The University of Auckland, New Zealand.

3. P Du is with the Auckland Bioengineering Institute and Department of Engineering Science, The University of Auckland, New Zealand. Email: peng.du@auckland.ac.nz

V (versus Ag/AgCl (3 M KCl)) using a PalmSens4 potentiostat. PEDOT:PSS coatings were deposited on each of the electrode by passing a varying level of charge: 0.3, 0.6, 0.9 and 1.2 mC, as shown in Fig. 1C. Each PEDOT:PSS coated electrode was paired with a neighboring Au electrode.

B. Experimental Recording

Ethical approval was granted by The University of Auckland Animal Ethics. HR mapping of the stomach was conducted in an acute manner using previously validated methods [12]. Three healthy white cross-breed weaner pigs (weight 42.4 ± 1.9 kg) were housed individually and fasted overnight before the experiments to avoid compounding effects of ingestion. Each subject was infused with 6% Voluven saline (Fresenius Kabi Freeflex, USA) and general anaesthesia with Zoletil (tiletamine HCl 50 mg mL^{-1} and zolazepam HCl 50 mg mL^{-1}) and isoflurane (2.5 – 5%) with an oxygen flow of 400 mL within a closed-circuit anesthetic system. Vital signs (blood pressure, heart rate, and temperature) were monitored continuously throughout the experiments. The femoral artery was cannulated in the right limb for blood pressure. A rectal thermometer was deployed to measure temperature. Endotracheal intubation was performed using Normocap 200 Oxy to monitor O_2, CO_2 and N_2O level. The subjects were maintained in a normal physiological range during the experiments by a respiration pump (Harvard Aparratus, co, Inc, USA) and a heating lamp (38.5 - 39.5 ºC).

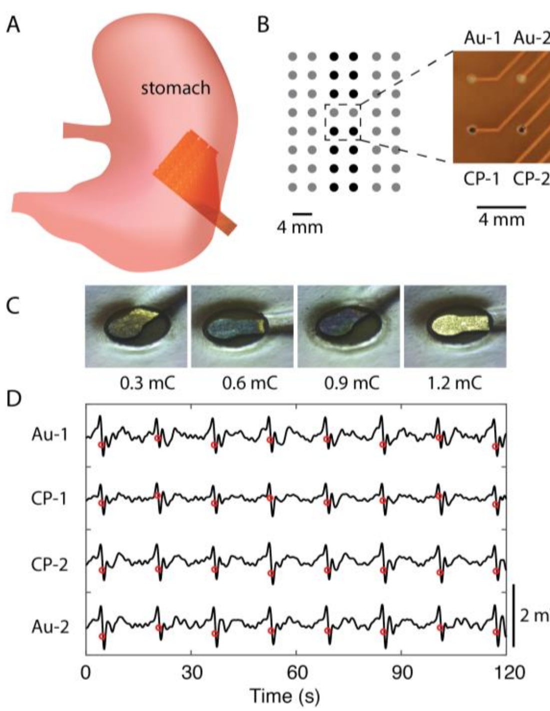

Fig 1. Experimental setup of the flexible electrode array over the anterior serosal surface of the stomach. (A) The position of the array. (B) The arrangement of the CP electrodes (black) and Au electrodes (gray). The zoomed in photo shows the covering of the PEDOT:PSS on top of the electrodes. (C) Photos of PEDOT:PSS coating under different levels of charges. (D) A sample electrograms of the neighboring CP and Au electrodes as indicated in (B). The red dots show the activation times of gastric slow waves identified by the down-stroke in the signal.

Following light skin preparation of the abdominal region using Nuprep (Weaver and Company), a mid-line laparotomy was performed to access the stomach of the subjects for HR mapping. One PEDOT:SS array was placed between two adjacent FPC arrays and inserted into the abdominal cavity to record gastric slow waves from the serosal surface of the gastric corpus directly (Fig. 1A). Each array was connected to the ActiveTwo system via a 32-way ribbon cable and a fiber-optic cable to a notebook. The incision was then sutured for the duration of the experiment. Signals were aquired at 512 Hz. At the conclusion of the studies, the subjects were euthanized with a bolus injection of 50 mL of magnesium sulfate.

C. Signal Processing

Signal processing and analysis were performed in MATLAB (R2019a, MathWorks). The serosal recordings were processed in the Gastric Electrical Mapping Suite (GEMS, The University of Auckland, New Zealand) [13]. Briefly, activation times of gastric slow waves were identified and grouped into individual cycles of gastric slow waves. The spatiotemporal characteristics were visualized as activation maps. The activation time of each gastric slow wave was automatically marked then grouped into discrete wavefronts (cycles), followed by manual review and correction. Regular antegrade propagation was classified as normal slow waves from the fundus to the antrum, as defined in a previous baseline study [14]. Spatial dysrhythmias were defined as directional deviations from the typical antegrade propagation. The average amplitude, velocity, derivative and interval from the preceding cycle were quantified for every cycle of analyzed slow waves.

The SNR analysis was performed following Kraiser windowing, equivalent noise bandwidth and periodogram on the active and passive electrodes. The SNR of the recorded slow waves was computed by integrating of power spectral density estimates of over a specific frequency (the area under the periodogram), using the following equation:

$$SNR = 20\log_{10}\left(\frac{P_{SW}}{P_N}\right) \quad (1)$$

where P_{SW} and P_N are the PSD estimates of the slow wave signals and noises.

Data from neighboring Au and PEDOT:PSS electrodes were paired, in order to eliminate the physiological variations in amplitude and velocity of slow waves in different regions of the stomach [14]. A p-value of less than 0.05 was considered to be statistically significant. A one-way ANOVA was then performed to explore any potential effects of the different deposition parameters. A Tukey-Kramer follow-up test was used to quantify the difference where statistical significance was found.

III. Results

Stable gastric slow waves were recorded in all subjects, covering an average recording period of 50 ± 16 minutes per subject. A total of 581 cycles of gastric slow waves were analyzed, with an average frequency of 3.78 ± 0.05 cycles per minute (cpm), amplitude of 1.30 ± 0.06 mV, velocity of 7.56 ± 0.22 mm s^{-1} and derivative of 2.68 ± 0.09 mV s^{-1}.

Both antegrade (n = 451) and retrograde (n = 129) propagating waves were recorded using the PEDOT:PSS and Au FPC arrays. In a normal stomach, the antegrade wave would propel ingested food towards the pyloric sphincter for further mixing or emptying into the small intestine. An example of an antegrade propagating wave is shown in Fig. 2A. The arrays were positioned on the posterior (back) serosal surface of the stomach. The activation map (Fig. 2A) reconstructed from the entire array demonstrated a propagation wavefront towards the pylorus of the stomach at an average frequency of 4.0 ± 0.2 cpm, amplitude of 1.41 ± 0.08 mV, velocity of 7.64 ± 0.28 mm s^{-1} and derivative of 2.97 ± 0.11 mV s^{-1}. The selected electrograms (Fig. 2C&D) demonstrated agreements in the direction of propagation registered by both types of electrodes.

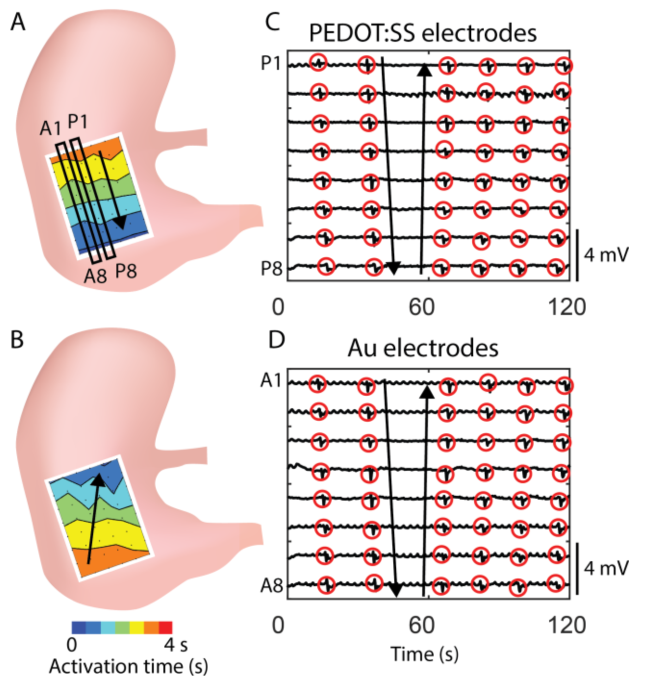

Fig 2. Example electrograms and activation sequence of gastric slow waves recorded using PEDOT:PSS and Au electrodes on a printed flexible HR mapping array. Directionality of antegrade (A) and retrograde (B) events was indicated by the arrows. The neighboring pairs of PEDOT:PSS (P1-8) and Au electrodes (A1-8) were selected (rectangle boxes) and their electrograms demonstrated in (C) and (D), respectively. The red dots indicate a detected slow wave event. The directionality of the slow waves in the electrograms is indicated by the solid arrows (down: antegrade, up: retrograde).

An example of a retrograde propagating wave is shown in Fig. 2B. The activation map reconstructed from the entire array demonstrated a propagation wavefront from the pylorus towards the fundus at an average frequency of 3.8 ± 0.2 cpm, amplitude of 1.18 ± 0.03 mV, velocity of 7.5 ± 0.14 mm s^{-1} and derivative of 2.39 ± 0.05 mV s^{-1}. Similar to the antegrade wavefront, both types of electrodes showed agreement in the direction of propagation and comparable signals (Fig. 2C&D).

The average of SNR of PEDOT:PSS was comparable with the Au electrodes (3.89 ± 2.62 vs 3.25 ±1.85 dB; p = 0.26). The performance of PEDOT:PSS in terms of frequency and velocity was also comparable with Au electrode pairs, as shown in Fig. 3A&C, respectively. In particular a large range of slow wave frequencies across both contact materials.

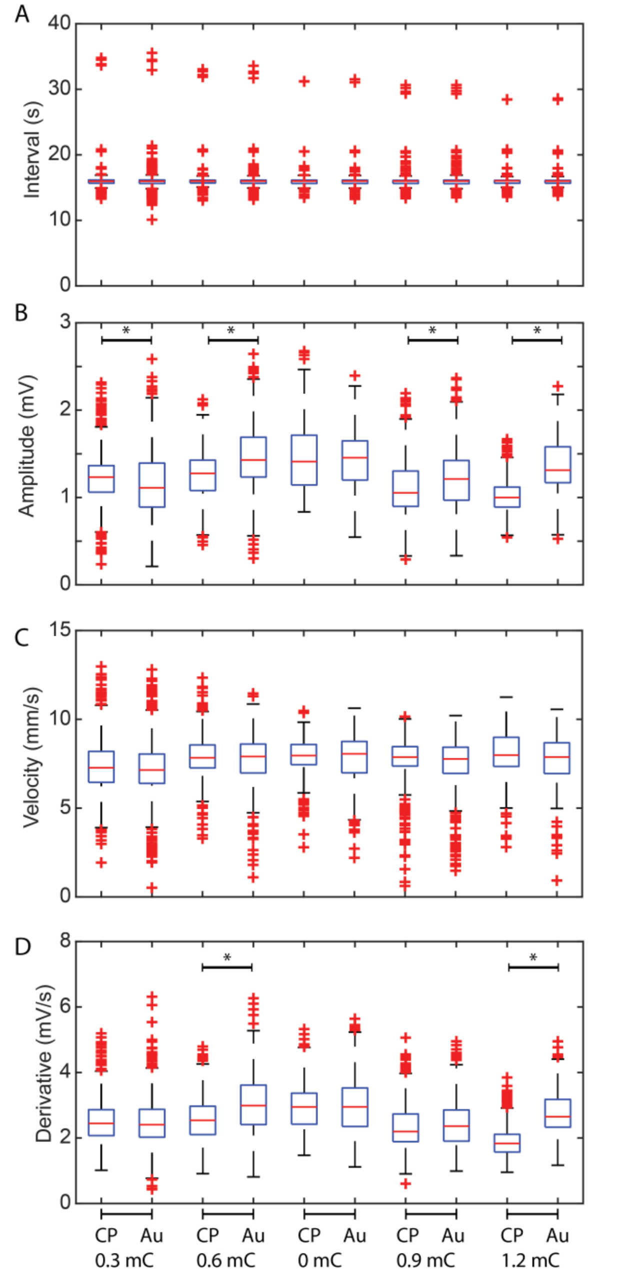

Fig 3. Summary data of the performance of PEDOT:PSS electrodes compared with the neighboring Au electrodes a varying levels of charge. The red crosses indicate outliers beyond the interquartile range. (A) Interval/frequency measure was identical in all pairs. (B) Amplitude showed differences in most electrode pairs. (C) Velocity measure was identical in all pairs. (D) Differences in the derivative of signals were detected at 0.6 mC and 1.2 mC compared with the Au electrodes. Black lines (*) indicate statistical significance ($p < 0.05$).

Amplitudes were generally lower in the PEDOT:PSS electrodes compared with the Au electrodes at all levels of charges used for PEDOT deposition, except at 0.3 mC (0.01-0.06 mV higher at 0.3 mC; 0.19 – 0.24 mV lower at 0.6 mC; 0.12 – 0.16 mV at 0.9 mC; and 0.35 – 0.41 mV lower at 1.2 mC). The derivatives were all different at two levels of charges: 0.58-0.48 mV/s lower at 0.6 mC and 0.87 – 1.02 mV/s at 1.2 mC.

IV. DISCUSSION

The performance of PEDOT:PSS coated electrodes were compared with Au coated electrodes for gastric slow wave recordings in acute recordings. The results demonstrated that the PEDOT:PSS is capable of adequately recording the frequency, amplitude and propagation of gastric slow waves. Furthermore, the conducting polymer deposition parameters affected the performance of the electrodes.

Both PEDOT:PSS and Au electrodes were able to register slow wave activation profiles in both antegrade and retrograde direction. Critically, both frequency and velocities were reliably detected by the PEDOT:PSS electrodes (Fig. 3A&C), with comparable SNR to the Au electodes. Further applications of the conducting polymer will include embedding the conductive connectors, instead of Au, into a flexible and compliant substrate, as well as use of CPs for measurements of strain/pressure for electromechanical analysis [15]. Given the stretchable substrate, the new conducting polymer sensors will be able to form and maintain good contact with the surface of the gastrointestinal tract, as has been demonstrated in cardiac research [16] and measure strains *in-situ*. Moreover, the PEDOT conducting polymer also has the potential to demonstrate a significantly promoted current injection density (~30 times higher) that platinum electrodes [17], which makes it ideal for high energy gastric pacing applications [18].

V. CONCLUSIONS

The performance of PEDOT:PSS electrodes was comparable to the standard Au electrodes for HR mapping of gastric slow waves, across all deposition parameters. Further applications will include embedding the CP conductive contacts into a flexible and compliant substrate, as well as CP-based strain sensors for electromechanical analysis.

REFERENCES

[1] J. D. Huizinga and W. J. Lammers, "Gut peristalsis is governed by a multitude of cooperating mechanisms," *Am. J. Physiol. Gastrointest. Liver Physiol.*, vol. 296, no. 1, pp. G1-8, 2009, doi: 10.1152/ajpgi.90380.2008.

[2] G. O'Grady, P. Du, L. K. Cheng, J. U. Egbuji, W. J. E. P. Lammers, J. A. Windsor, and A. J. Pullan, "Origin and propagation of human gastric slow-wave activity defined by high-resolution mapping\," *Am. J. Physiol. Liver Physiol.*, vol. 299, no. 3, pp. G585–G592, Sep. 2010, doi: 10.1152/ajpgi.00125.2010.

[3] D. A. Carson, G. O'Grady, P. Du, A. A. Gharibans, and C. N. Andrews, "Body surface mapping of the stomach: New directions for clinically evaluating gastric electrical activity.," *Neurogastroenterol. Motil.*, p. e14048, Dec. 2020, doi: 10.1111/nmo.14048.

[4] W. J. Lammers, A. el-Kays, K. Arafat, and T. Y. el-Sharkawy, "Wave mapping: detection of co-existing multiple wavefronts in high-resolution electrical mapping," *Med. Biol. Eng. Comput.*, vol. 33, no. 3 Spec No, pp. 476–481, 1995, [Online]. Available: http://www.ncbi.nlm.nih.gov/pubmed/7666697.

[5] P. Du, G. O'Grady, J. U. Egbuji, W. J. Lammers, D. Budgett, P. Nielsen, J. A. Windsor, A. J. Pullan, and L. K. Cheng, "High-resolution mapping of in vivo gastrointestinal slow wave activity using flexible printed circuit board electrodes: methodology and validation," *Ann. Biomed. Eng.*, vol. 37, no. 4, pp. 839–846, 2009, doi: 10.1007/s10439-009-9654-9.

[6] G. O'Grady, T. H. H. Wang, P. Du, T. Angeli, W. J. Lammers, and L. K. Cheng, "Recent progress in gastric arrhythmia: Pathophysiology, clinical significance and future horizons," *Clin. Exp. Pharmacol. Physiol.*, vol. 41, no. 10, pp. 854–862, 2014, doi: 10.1111/1440-1681.12288.

[7] G. O'Grady, N. Paskaranandavadivel, T. R. Angeli, P. Du, J. A. Windsor, L. K. Cheng, and A. J. Pullan, "A comparison of gold versus silver electrode contacts for high-resolution gastric electrical mapping using flexible printed circuit board arrays," *Physiol. Meas.*, vol. 32, no. 3, 2011, doi: 10.1088/0967-3334/32/3/N02.

[8] E. Tomaskovic-Crook, P. Zhang, A. Ahtiainen, H. Kaisvuo, C.-Y. Lee, S. Beirne, Z. Aqrawe, D. Svirskis, J. Hyttinen, G. G. Wallace, J. Travas-Sejdic, and J. M. Crook, "Human Neural Tissues from Neural Stem Cells Using Conductive Biogel and Printed Polymer Microelectrode Arrays for 3D Electrical Stimulation.," *Adv. Healthc. Mater.*, vol. 8, no. 15, p. e1900425, 2019, doi: 10.1002/adhm.201900425.

[9] A. Akbarinejad, C. L. Hisey, D. Brewster, J. Ashraf, V. Chang, S. Sabet, Y. Nursalim, V. Lucarelli, C. Blenkiron, L. Chamley, D. Barker, D. E. Williams, C. W. Evans, and J. Travas-Sejdic, "Novel Electrochemically Switchable, Flexible, Microporous Cloth that Selectively Captures, Releases, and Concentrates Intact Extracellular Vesicles.," *ACS Appl. Mater. Interfaces*, vol. 12, no. 35, pp. 39005–39013, Sep. 2020, doi: 10.1021/acsami.0c11908.

[10] M. Gerard, A. Chaubey, and B. D. Malhotra, "Application of conducting polymers to biosensors.," *Biosens. Bioelectron.*, vol. 17, no. 5, pp. 345–59, May 2002, doi: 10.1016/s0956-5663(01)00312-8.

[11] M. Wang, P. Baek, A. Akbarinejad, D. Barker, and J. Travs-Sejdic, "Conjugated Polymers and Composites for Stretchable Organic Electronics," *J. Mater. Chmistry C*, no. 19, pp. 5534–5552, 2019.

[12] H. P. Simonian, K. Panganamamula, H. P. Parkman, X. Xu, J. Z. Chen, G. Lindberg, H. Xu, C. Shao, M.-Y. Ke, M. Lykke, P. Hansen, B. Barner, and H. Buhl, "Multichannel electrogastrography (EGG) in normal subjects: a multicenter study.," *Dig. Dis. Sci.*, vol. 49, no. 4, pp. 594–601, Apr. 2004, doi: 10.1023/b:ddas.0000026304.83214.50.

[13] R. Yassi, G. O'Grady, N. Paskaranandavadivel, P. Du, T. R. Angeli, A. J. Pullan, L. K. Cheng, and J. C. Erickson, "The gastrointestinal electrical mapping suite (GEMS): Software for analyzing and visualizing high-resolution (multi-electrode) recordings in spatiotemporal detail," *BMC Gastroenterol.*, vol. 12, 2012, doi: 10.1186/1471-230X-12-60.

[14] J. U. Egbuji, G. O'grady, P. Du, L. K. Cheng, W. J. Lammers, J. A. Windsor, and A. J. Pullan, "Origin, propagation and regional characteristics of porcine gastric slow wave activity determined by high-resolution mapping," *Neurogastroenterol. Motil.*, vol. 22, no. 10, pp. e292-300, 2010, doi: 10.1111/j.1365-2982.2010.01538.x.

[15] M. Wang, S. Kee, P. Paek, M. S. Ting, Z. Zujovic, D. Barker, and J. Travas-Sejdic, "Photo-patternable, stretchable and electrically conductive graft copolymers of poly(3-hexylthiophene)," *Polym. Chem.*, vol. 10, pp. 6278–6289, 2017.

[16] J. Liu, X. Zhang, Y. Liu, M. Rodrigo, P. D. Loftus, J. Aparicio-Valenzuela, J. Zheng, T. Pong, K. J. Cyr, M. Babakhanian, J. Hasi, J. Li, Y. Jiang, C. J. Kenney, P. J. Wang, A. M. Lee, and Z. Bao, "Intrinsically stretchable electrode array enabled in vivo electrophysiological mapping of atrial fibrillation at cellular resolution.," *Proc. Natl. Acad. Sci. U. S. A.*, vol. 117, no. 26, pp. 14769–14778, 2020, doi: 10.1073/pnas.2000207117.

[17] Y. Liu, J. Li, S. Song, J. Kang, Y. Tsao, S. Chen, V. Mottini, K. McConnell, W. Xu, Y.-Q. Zheng, J. B.-H. Tok, P. M. George, and Z. Bao, "Morphing electronics enable neuromodulation in growing tissue.," *Nat. Biotechnol.*, vol. 38, no. 9, pp. 1031–1036, 2020, doi: 10.1038/s41587-020-0495-2.

[18] R. Wang, Z. Abukhalaf, A. Javan-Khoshkholgh, T. H.-H. Wang, S. Sathar, P. Du, T. R. Angeli, L. K. Cheng, G. O'Grady, N. Paskaranandavadivel, and A. Farajidavar, "A Miniature Configurable Wireless System for Recording Gastric Electrophysiological Activity and Delivering High-Energy Electrical Stimulation.," *IEEE J. Emerg. Sel. Top. circuits Syst.*, vol. 8, no. 2, pp. 221–229, Jun. 2018, doi: 10.1109/JETCAS.2018.2812105.